An accuracy assessment of the MTBS burned area product for shrub–steppe fires in the northern Great Basin, United States

Article *in* International Journal of Wildland Fire · January 2015

Impact Factor: 2.43 · DOI: 10.1071/WF14131

6 authors, including:

Luigi Boschetti
University of Idaho
67 PUBLICATIONS **1,732** CITATIONS
SEE PROFILE

Alistair Matthew Stuart Smith
University of Idaho
94 PUBLICATIONS **2,165** CITATIONS
SEE PROFILE

Wade T. Tinkham
Colorado State University
18 PUBLICATIONS **166** CITATIONS
SEE PROFILE

Beth Newingham
United States Department of Agriculture
43 PUBLICATIONS **1,539** CITATIONS
SEE PROFILE

CSIRO PUBLISHING

International Journal of Wildland Fire **2015**, *24*, 70–78
http://dx.doi.org/10.1071/WF14131

An accuracy assessment of the MTBS burned area product for shrub–steppe fires in the northern Great Basin, United States

Aaron M. Sparks[A], *Luigi Boschetti*[A], *Alistair M. S. Smith*[A,B], *Wade T. Tinkham*[A], *Karen O. Lannom*[A] *and Beth A. Newingham*[A]

[A]Department of Forest, Rangeland, and Fire Sciences, University of Idaho, Moscow, ID 83844-1133, USA.
[B]Corresponding author. Email: alistair@uidaho.edu

Abstract. Although fire is a common disturbance in shrub–steppe, few studies have specifically tested burned area mapping accuracy in these semiarid to arid environments. We conducted a preliminary assessment of the accuracy of the Monitoring Trends in Burn Severity (MTBS) burned area product on four shrub–steppe fires that exhibited varying degrees of within-fire patch heterogeneity. Independent burned area perimeters were derived through visual interpretation and were used to cross-compare the MTBS burned area perimeters with classifications produced using set thresholds on the Relativised differenced Normalised Burn Index (RdNBR), Mid-infrared Burn Index (MIRBI) and Char Soil Index (CSI). Overall, CSI provided the most consistent accuracies (96.3–98.6%), with only small commission errors (1.5–4.4%). MIRBI also had relatively high accuracies (92.2–97.9%) and small commission errors (2.1–10.8%). The MTBS burned area product had higher commission errors (4.3–15.5%), primarily due to inclusion of unburned islands and fingers within the fire perimeter. The RdNBR burned area maps exhibited lower accuracies (92.9–96.0%). However, the different indices when constrained by the MTBS perimeter provided variable results, with CSI providing the highest and least variable accuracies (97.4–99.1%). Studies seeking to use MTBS perimeters to analyse trends in burned area should apply spectral indices to constrain the final burned area maps. The present paper replaces a former paper of the same title (http://dx.doi.org/10.1071/WF13206), which was withdrawn owing to errors discovered in data analysis after the paper was accepted for publication.

Additional keywords: CSI, dNBR, MIRBI, RdNBR, remote sensing.

Received 25 July 2014, accepted 28 August 2014, published online 26 November 2014

Introduction

Shrub–steppes are semiarid to arid lands dominated by shrubs with intermixed grasses and forbs that are sustained through ecological processes such as fire, drought and species succession (Stringham *et al.* 2003; Lund 2007; Abatzoglou and Kolden 2011). Although fire is an important disturbance agent in North American shrub–steppe systems, its historic prevalence has been less than in forests due to low plant cover and thus gaps in continuous surface vegetation to carry fire (West and Young 2000). Steppe fires can alter nutrient availability, promote the establishment of seral species and alter wildlife habitats (Crawford *et al.* 2004; Chambers *et al.* 2007). Area burned assessments in these ecosystems are necessary for land management personnel to effectively target and allocate resources to rehabilitation and restoration efforts (Baker 2006). We recognise that moderate spatial resolution sensors (e.g. MODIS: 0.25–1.0-km pixels) may continue to be used for global area burned mapping assessments (Roy *et al.* 2008); however, high spatial resolution datasets (i.e. Landsat-type sensors: 30-m pixels) will likely remain the most commonly applied by land and fire management personnel due to the spatial detail they provide (Lentile *et al.* 2006).

The Monitoring Trends in Burn Severity (MTBS) project was initiated with the objective of producing systematic, multi-year burned area maps and associated burn severity information over the United States, with a primary focus on land management support (Eidenshink *et al.* 2007). The product is generated with a semi-automated process, but limited validation of the MTBS maps, or similar perimeters have been presented in the literature (Brewer *et al.* 2005; Holden *et al.* 2005; Sunderman and Weisberg 2011; Kolden *et al.* 2012). However, accuracy assessment of the MTBS maps is essential given these data have been widely used for the characterisation of area burned and temporal analysis of regional area burned trends (Dillon *et al.* 2011; Zheng *et al.* 2011; Morton *et al.* 2012; Randerson *et al.* 2012; Riley *et al.* 2013; Lannom *et al.* 2014). The objective of

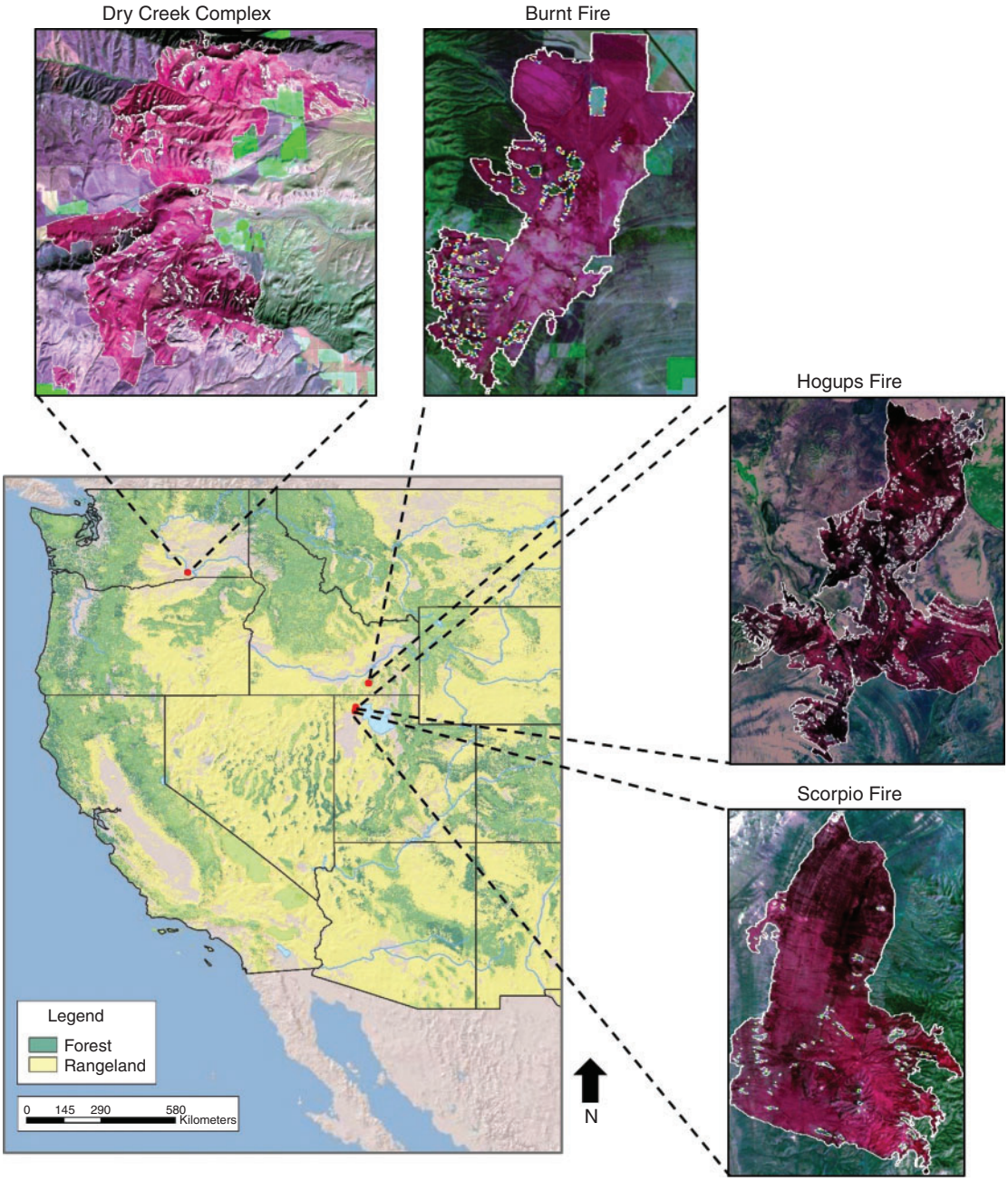

Fig. 1. Map of western United States forested and rangeland extent, which include shrub–steppe, and the location of the investigated fires (Burnt, Dry Creek Complex, Hogups and Scorpio). The Burnt Fire burned 3499 ha in south-central Idaho in early July, the Dry Creek Complex burned 18 592 ha in south-central Washington, the Hogups fire burned 10 425 ha in north-west Utah in early August and the Scorpio fire burned 5789 ha in north-west Utah in late June. (colour)

this study was to conduct a comparative assessment of the semi-automated area burned maps produced by the MTBS project as applied to shrub–steppe fires. The specific questions we sought to address for the MTBS area burned product were:

(1) What is the areal accuracy of the burned area MTBS polygons?
(2) Can the accuracy be improved by applying a simple threshold to spectral indices within the polygons?

Datasets

Study area and imagery

For this preliminary study, we selected four shrub–steppe fires that burned in the summer of 2006 and 2009 in the Great Basin, United States (Fig. 1). The fires all burned in similar Great Basin vegetation types characterised by patchy sagebrush (*Artemisia* spp.), bunchgrasses (e.g., Sandberg bluegrass, Poa secunda and bluebunch wheatgrass), Pseudoroegneria spicata and annual

invasive grasses, including cheatgrass (*Bromus tectorum*). The Burnt Fire burned mostly in the sagebrush and grass vegetation on the edge of the Black Pine Mountains of Idaho and expanded to several adjacent agriculture fields. The Hogups and Scorpio fires burned in grass and sagebrush vegetation in the Hogups Mountains north-east of the Great Salt Lake, Utah. The Dry Creek Complex Fire burned mostly in grass and sagebrush near the Columbia River 9.8 km north of Sunnyside, Washington State. These four fires were selected as they visually exhibited different degrees of within-fire patch heterogeneity. The Scorpio Fire produced large tracts of area burned with few unburned patches, whereas the Hogups and Dry Creek Complex fires each produced many unburned islands within the perimeter, as well as numerous burned 'fingers' that extend from the main body of area burned. The Burnt Fire represents the intermediate scenario, with a small number of unburned patches.

The fires are covered by Landsat path 39 row 31 (Burnt, Hogups and Scorpio fires) and Landsat path 45 row 28 (Dry Creek Complex). Landsat 5 TM imagery was selected, because since 2003, Landsat 7 ETM+ images are affected by the failure of the Scan Line Corrector (SLC) and are unsuitable for mapping ephemeral land cover changes, such as fires. The selected Landsat 5 images were acquired on 15 July 2006 (Scorpio), 16 August 2006 (Burnt and Hogups), and 5 October 2009 (Dry Creek Complex). Calibration and atmospheric correction for each scene was performed using the Landsat Ecosystem Disturbance Adaptive Processing Systems (LEDAPS) (Masek *et al.* 2006, 2008). The images were subset to the minimum enclosing rectangle around each fire.

We also acquired post-fire aerial imagery from the National Agriculture Imagery Program (NAIP) for the Burnt (21 July 2006), Scorpio (27 August 2006), and Hogups (27 August 2006) fires. No NAIP data were available for the 2009 Dry Creek fire. NAIP imagery consists of orthorectified visible (red, green, blue) un-calibrated digital aerial photographs with spatial resolution of 1 m (Scorpio and Hogups) or 2 m (Burnt).

MTBS products

The MTBS project develops area burned and severity maps across all lands of the United States from 1984 onwards, using Landsat imagery. All fires larger than ~2 km^2 (500 acres) are mapped in the eastern United States and ~4 km^2 (1000 acres) in the western United States. The available products include:

- fire perimeters, distributed in vector format (ESRI shape file)
- pre-fire and post-fire Landsat TM/ETM+ raster images, clipped to a 3-km buffered box around each fire perimeter
- NBR, dNBR and RdNBR spectra index rasters, clipped to a 3-km buffered box around each fire perimeter
- thematic burn severity map with five severity classes, defined for each pixel within a fire perimeter.

In the present study we used two of the MTBS products: the fire perimeters and the RdNBR images. The fire perimeters are defined by analysts who rapidly and manually digitise the Landsat dNBR imagery. The polygons exhibit a degree of simplification of the fire perimeter and, by project requirement, do not identify any unburned islands within the perimeter. RdNBR was developed by Miller and Thode (2007) as a relativised version of dNBR that normalises for the pre-fire vegetation. $RdNBR = dNBR \div \sqrt{(NBR_{prefire}/1000)}$, $dNBR = NBR_{pre} - NBR_{post}$, $NBR = (\rho_4 - \rho_7) \div (\rho_4 + \rho_7)$, where ρ_i denotes the surface reflectance of Landsat band *i*. Although dNBR was developed for assessing post-fire effects and will not be ideal for assessing burned and unburned pixels (Verstraete and Pinty 1996; Pereira *et al.* 1999; Smith *et al.* 2007*a*; Lentile *et al.* 2009; Heward *et al.* 2013), its classification schema does include an unburned-to-low severity category and therefore we sought to explore its utility in addressing question (2). The RdNBR images of each fire were produced following Miller and Thode (2007). Within MTBS, dNBR severity classes (unburned-to-low, low-to-moderate and moderate-to-high) are manually identified for each fire using interpretations of the dNBR and RdNBR data, raw pre- and post-fire satellite imagery, plot data (if available) and the analyst's own judgment Eidenshink *et al.* (2007).

Methods

Spectral index area burned maps

Semi-manual area burned maps were derived for the four fires by applying thresholds to spectral indices previously used in similar environments: RdNBR, the Mid-infrared Burn Index (MIRBI) (Trigg and Flasse 2001; Smith *et al.* 2007*b*) and the Char Soil Index (CSI) (Smith *et al.* 2005).

MIRBI was originally formulated for MODIS data and is a linear combination of MODIS Band 6 (1.63–1.65 μm) and 7 (2.10–2.15 μm); the index was designed to have isolines orthogonal to the spectral changes induced by fire and appears insensitive to vegetation type (Trigg and Flasse 2001). Smith *et al.* (2007*b*) tested the broader applicability of this method using Landsat TM/ETM+ imagery and demonstrated that in savannah systems MIRBI, alongside linear spectral unmixing, outperformed other tested approaches. The general formulation of MIRBI for Landsat imagery is: $MIRBI = 10*\rho_7 - 9.8*\rho_5 + 2.0$, where ρ_7 = TM Band 7 reflectance (2.08–2.35 μm) and ρ_5 = TM Band 5 reflectance (1.55–1.75 μm) (Smith *et al.* 2007*b*). Given past studies indicating that MIRBI thresholds around 2.0 provided optimal discrimination of burned from unburned areas, our analysis began at this threshold and sequentially evaluated alternative thresholds at 0.05 intervals. An optimal threshold was selected for each study area by selecting the value that produced the most accurate classification when compared with the reference imagery described in the next section.

The Char Soil Index (CSI), defined as ρ_4/ρ_5, i.e. the simple ratio of ρ_4 = TM Band 4 reflectance (0.76–0.90 μm) and ρ_5 = TM Band 5 reflectance (1.55–1.75 μm). CSI was developed by Smith *et al.* (2005) and consequently applied in several studies (Smith *et al.* 2007*b*; Stroppiana *et al.* 2012) that demonstrated it to be an effective area burned mapping approach in both savannah and Mediterranean ecosystems. Following the MIRBI process, optimal CSI and RdNBR thresholds were also determined.

For each spectral index approach we additionally constrained the resultant burned or unburned classification by the MTBS perimeter to evaluate the potential of a coupled (MTBS perimeter + index) approach.

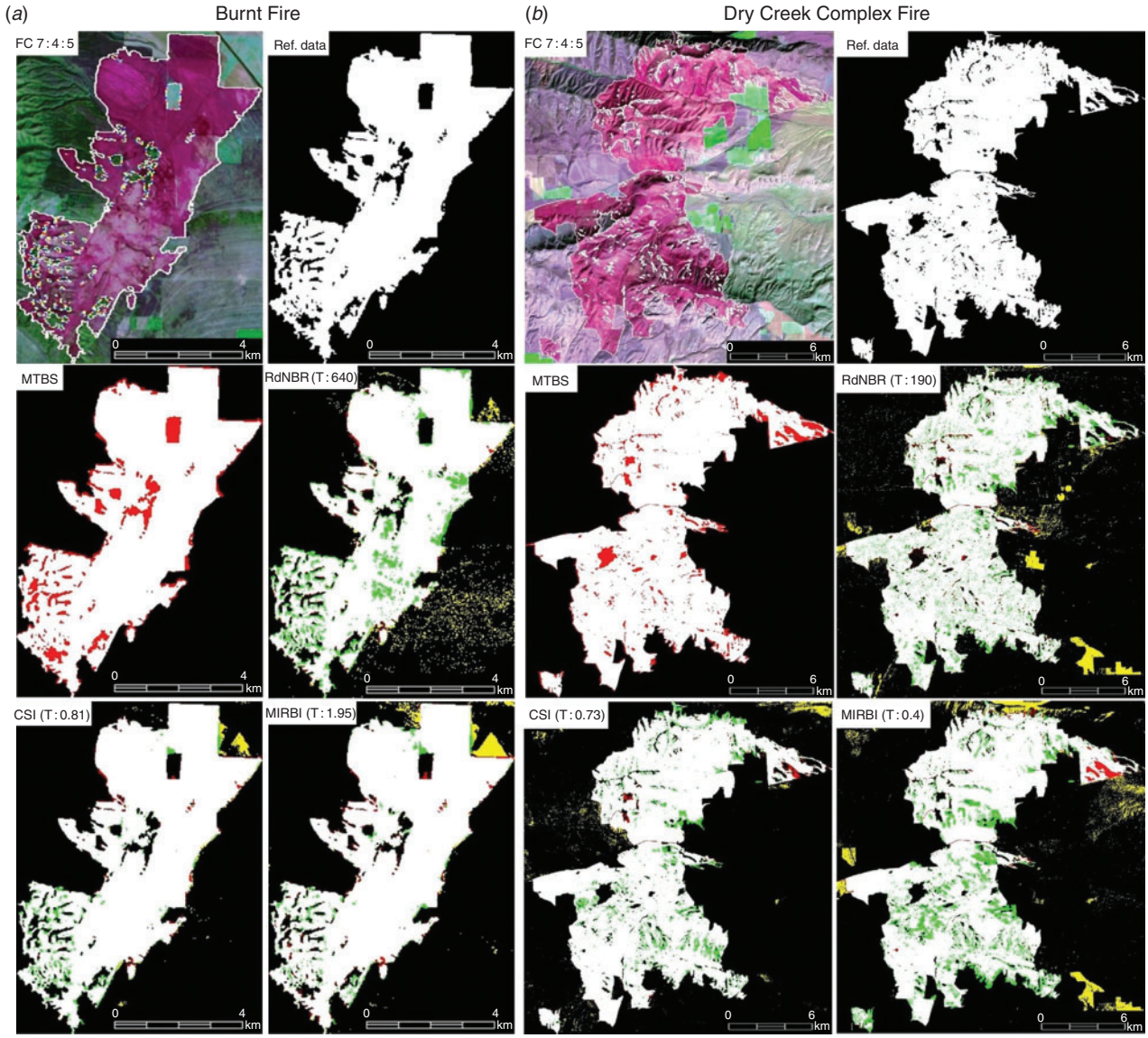

Fig. 2. Remote sensing imagery for the (*a*) Burnt Fire and (*b*) Dry Creek Complex Fire showing a Landsat TM false colour (FC) composite (R: Band 7, G: Band 4, B: Band 5), the visually interpreted reference data (Ref. data), MTBS perimeter with commission errors shown in red, and RdNBR (Relativised differenced Normalised Burn Ratio), CSI (Char Soil Index) and MIRBI (Mid-infrared Burn Index) burned area maps displaying correctly classified burned area (white) and non-burned area (black), commission (red) and omission errors (green) inside the burn perimeter, and commission errors (yellow) outside the burn perimeter. Threshold values used for the classification are reported for each index. (colour)

Reference data

Key to any robust accuracy assessment is the application of representative, independent validation reference data that are inherently more accurate than the product to be evaluated (Smith *et al.* 2002; Boschetti *et al.* 2006; Olofsson *et al.* 2013, 2014). Although ground data and aerial surveys can potentially yield reference data that are more accurate than high-resolution remote sensing data, their potential use for retrospectively validating burned area products is very limited as the collection of new data is, by definition, impossible.

Consequently, the use of remotely sensed data as reference is in many cases the only viable option: the international Global Burned Area Satellite Validation Protocol, endorsed by the Committee on Earth Observation Satellites (CEOS), requires that when satellite data are used as reference data they should (A) ideally have a higher spatial resolution than the data used to generate the area burned product, (B) exhibit spectral and radiometric resolution adequate for the unambiguous discrimination of burned from unburned areas, and (C) be acquired before any vegetation recovery or removal of char and ash; that is, within weeks after the fire event in savannah and grassland ecosystems (Boschetti *et al.* 2009; Picotte and Robertson 2011).

Those conditions can usually be met for the validation of coarser resolution (250–1000 m), where Landsat-derived maps are used as reference dataset. However, when Landsat resolution burned area maps are used as the classification dataset, it is

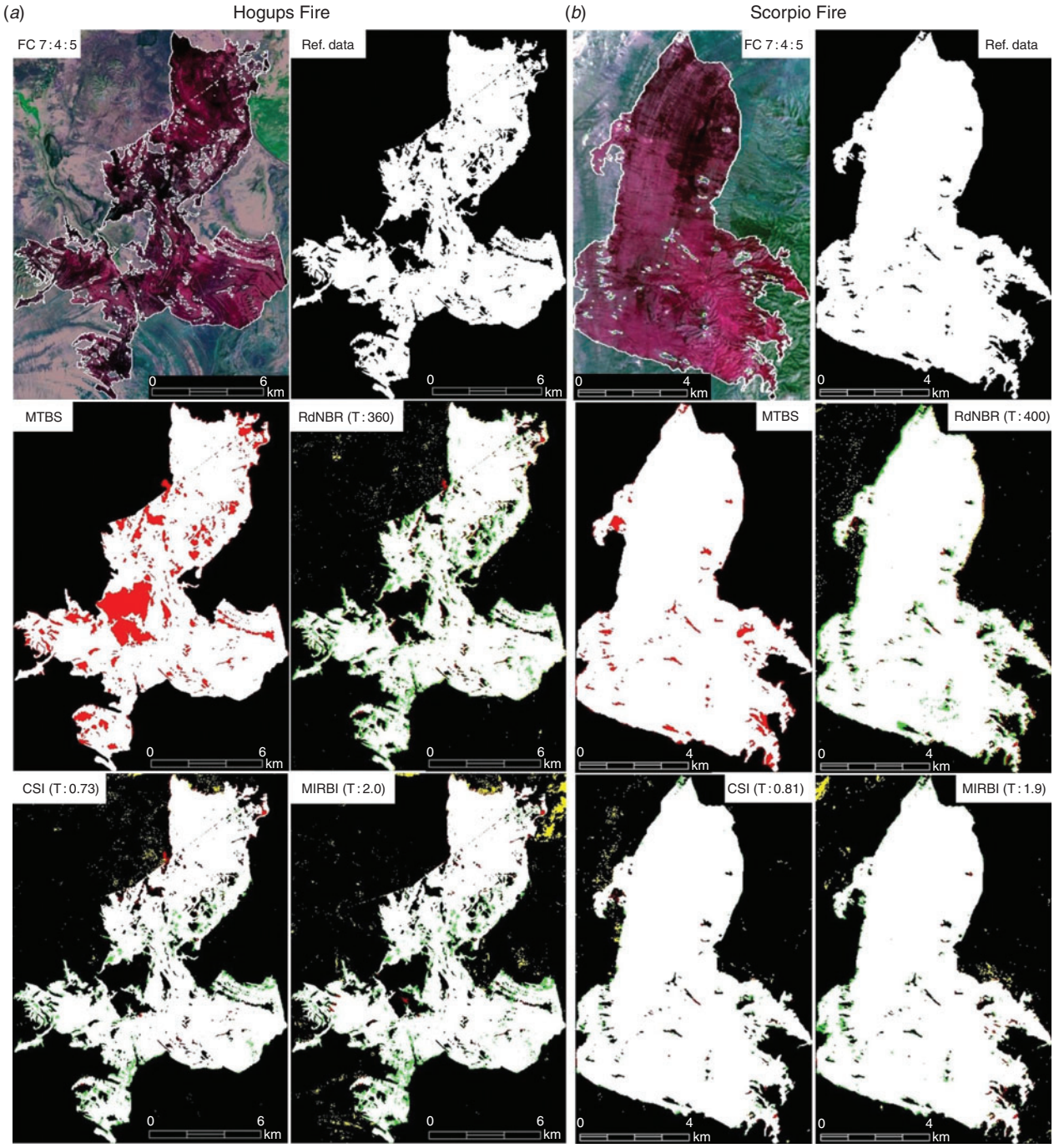

Fig. 3. Remote sensing imagery for the (*a*) Hogups Fire and (*b*) Scorpio Fire showing a Landsat TM false colour (FC) composite (R: Band 7, G: Band 4, B: Band 5), the visually interpreted reference data (Ref. data), MTBS perimeter with commission errors shown in red, and RdNBR (Relativised differenced Normalised Burn Ratio), CSI (Char Soil Index) and MIRBI (Mid-infrared Burn Index) burned area maps displaying correctly classified burned area (white) and non-burned area (black), commission (red) and omission errors (green) inside the burn perimeter, and commission errors (yellow) outside the burn perimeter. Threshold levels are inset for each of the indices. (colour)

problematic to find higher-resolution reference data. This is because imagery with very high spatial resolution (i.e. 1–4 m) is only sporadically available, and often does not have sufficient spectral resolution to allow for the unambiguous identification of burned areas. For instance, most aerial and satellite very-high-resolution sensors acquire visible and panchromatic imagery, which provides very poor discrimination between dark soil, dark vegetation and burned areas.

Given the lack of higher-resolution imagery, visual interpretation of Landsat images has been often used to provide

Table 1. Burned area accuracy assessment of the MTBS burned area perimeter (column 1), the spectral index burned area maps (columns 2–5), and the CSI, MIRBI, dNBR and RdNBR classifications constrained by MTBS perimeters for the four fires (columns 6–9)
All accuracies are expressed as percentages. CSI, Char Soil Index; MIRBI, Mid-infrared Burn Index; RdNBR, Relativised differenced Normalised Burn Ratio

Fires		MTBS perimeters	Maps from Index constrained to MTBS perimeters				Maps from index threshold			
			CSI	MIRBI	dNBR	RdNBR	CSI	MIRBI	dNBR	RdNBR
Burnt	Method threshold	n/a	0.81	1.95	135	640	0.81	1.95	135	640
	Overall accuracy	95.4	98.0	97.3	92.3	92.9	98.1	97.6	95.7	95.1
	Commission burned	10.1	2.6	6.6	12.0	8.1	1.5	2.5	3.9	2.3
	Commission unburned	0.2	1.7	1.1	4.4	6.5	2.3	2.3	4.5	6.5
	Omission burned	0.3	4.1	2.8	6.2	9.7	3.4	3.4	6.8	10.1
	Omission unburned	7.3	1.0	2.6	8.7	5.4	1.0	1.7	2.6	1.4
	Total area burned (bias, %)	5.3	−0.02	−1.2	6.6	−1.7	−2.6	−1.0	−3.3	−8.0
Dry Creek	Method threshold	n/a	0.73	0.4	70	190	0.73	0.4	70	190
	Overall accuracy	96.9	96.3	92.2	94.1	93.9	97.4	95.1	97.1	95.6
	Commission burned	8.3	4.4	10.8	10.6	10.3	1.2	2.2	2.5	2.6
	Commission unburned	0.1	3.4	6.4	3.3	4.0	3.2	6.0	3.2	5.1
	Omission burned	0.3	6.8	12.7	6.3	7.7	6.6	12.5	6.4	10.6
	Omission unburned	4.6	2.2	5.3	5.6	5.3	0.6	1.0	1.2	1.2
	Total area burned (bias, %)	8.8	−2.5	−2.2	4.9	−0.2	−5.7	−10.8	−4.0	−8.2
Hogups	Method threshold	n/a	0.73	2.0	150	360	0.73	2.0	150	360
	Overall accuracy	94.2	97.2	95.8	93.3	94.9	97.8	97.2	94.3	96.9
	Commission burned	15.5	3.8	7.4	7.0	6.6	2.0	1.7	3.6	0.0
	Commission unburned	0.4	2.3	2.9	6.6	4.4	2.3	3.3	6.7	4.3
	Omission burned	0.9	5.2	7.5	13.2	10.1	4.7	7.6	13.6	10.1
	Omission unburned	8.0	1.7	2.9	3.4	2.8	1.0	0.7	1.7	0.0
	Total area burned (bias, %)	16.8	−1.4	−1.1	−6.8	−3.8	−3.7	−6.1	−10.5	−10.1
Scorpio	Method threshold	n/a	0.81	1.9	150	400	0.81	1.9	150	400
	Overall accuracy	97.6	98.6	97.9	94.3	96.0	99.1	98.4	95.8	96.7
	Commission burned	4.3	1.5	2.1	3.2	3.3	0.7	0.9	0.0	1.8
	Commission unburned	0.4	1.3	2.2	8.0	4.7	1.2	2.3	7.8	4.7
	Omission burned	0.4	1.3	2.2	8.4	4.7	1.2	2.3	8.4	4.8
	Omission unburned	4.5	1.6	2.1	3.1	3.3	0.7	0.9	0	1.7
	Total area burned (bias, %)	4.1	0.2	−0.1	−5.3	−1.4	−1.3	−1.4	−8.4	−1.6

reference data (Brewer *et al.* 2005; Petropoulos *et al.* 2010; Oliveira *et al.* 2012; Stroppiana *et al.* 2012). Visual interpretation of the Landsat data by a well-trained expert generally yields the most accurate results and can be assumed to be the best possible classification of the input data against which the performance of automatic classification algorithms can be compared. Cross-checking of such assessments by another expert can help reduce subjectivity. When reference data do not span the entire feature being evaluated or when it is too costly to obtain comprehensive reference imagery, statistical sampling methods are used (Smith *et al.* 2002; Olofsson *et al.* 2013, 2014).

In the current study we created our reference data via visual interpretation of false colour composites (Landsat Bands 7 : 4 : 5, Fig. 1 and Bands 7 : 4 : 3); the 1–2-m NAIP aerial imagery did not have sufficient spectral resolution to discriminate reliably between burned and unburned areas, but was used as an additional data source to aid the interpreter in the visual interpretation of the Landsat data. The digitisation was conducted on a pixel-by-pixel basis, thus avoiding any simplification of the polygon boundaries. As a result of the visual interpretation, each pixel of the selected study areas (>1 million per fire) was classified as either burned or unburned. Uncertain pixels at the edges of the area burned were alternately classified as burned or unburned. The confusion matrix between the reference data, the rasterised MTBS polygons and the six maps obtained from the spectral indices (two maps per index, one applied to the whole study area, and one constrained to the MTBS polygons) was used to calculate overall accuracy, omission and commission errors, and total area burned bias.

Results and discussion

Accuracy of burned area MTBS polygons

Figs 2 and 3 show, for the four fires, the reference perimeters overlaid on a Landsat post-fire false-colour composite, as well as the MTBS fire polygons and the raster maps obtained by thresholding the three spectral indices. In each of Figs 2 and 3 the colours indicate agreement and disagreement between the reference data and the classification: commission errors inside and outside the fire perimeter are plotted in red and yellow; correctly classified burned and unburned areas are plotted in white and black; omission errors are plotted in green. The accuracy metrics obtained from the confusion matrix are reported in Table 1. The MTBS perimeters had overall accuracies across all four fires ranging from 94.2 to 97.6% (Table 1).

However, as evident in Figs 2 and 3, the MTBS perimeters often oversimplify the burned area polygons when the areas are very fragmented and do not map large unburned islands. This causes a significant bias in area burned: the MTBS perimeters overestimated the area burned on all fires, by a percentage between 4.1 and 16.8%.

Accuracy of spectral index-based burned area maps

The burned area maps obtained through applying RdNBR on the whole image had moderate burned area commission (3.3–10.3%) and omission (4.7–10.1%) errors evident in Figs 2 and 3, and consequently balancing the area burned bias (−0.2 to −3.8%). Application of the MIRBI spectral index, with an individual optimal threshold determined for each fire, provided overall accuracies of area burned ranging from 92.2 to 97.9% (Table 1), with the omission and commission errors resulting in slight underestimations of the total area burned (−0.1 to −2.2%). Across all four fires, the MIRBI thresholds produced a burned commission error of 2.1–10.8% (Table 1). The CSI spectral index produced accuracies of area burned ranging from 96.3 to 98.6% (Table 1), with low omission and commission errors (Figs 2*a* and 3*b*) and small over or under estimation of area burned (<3%). The slight difference in performance between the three spectral indices can be explained given the RdNBR was never intended to be used outside the burn perimeter. In contrast, the CSI and MIRBI indices were developed by optimising the spectral separation between unburned and burned surfaces in each study site (Trigg and Flasse 2001; Smith *et al.* 2005).

Accuracy of spectral index maps constrained by MTBS polygons

Constraining the RdNBR spectral index by the MTBS perimeters did not improve the accuracy for the four fires, with the bias shifting from positive (+4.1 to +16.8%) to negative (−1.6 to −10.1%). When constrained by the MTBS perimeter, MIRBI showed slight increases in accuracy for all fires. As can be expected, the constrained maps exhibited lower burned commission errors (0.9–2.5%). However, because of the significant omission error, the total burned area was underestimated (−1.0 to −10.8%, Table 1). Constraining the CSI map by the MTBS polygons provided the highest accuracy of the three spectral indices. Overall, the CSI spectral index was the most consistent when producing accurate burned area maps. When evaluating the data across the four fires, the CSI index on average increased the accuracy between 1.5 and 2.0% over the MTBS perimeter product. All the explored methods decreased the absolute bias (1.8–7.7%) when compared with the MTBS perimeter product. This illustrates that the burned–unburned thresholds provided by spectral indices could be used to generate an alternative burned area map. In a similar manner to Abatzoglou and Kolden (2013) who excluded the unburned-to-low severity class from the MTBS perimeters, at a minimum these spectral index thresholds could be used to further refine the vector MTBS polygons. This study did evaluate subtracting the unburned-to-low dNBR class from the MTBS polygon, but the resultant accuracies (94.3–97.1%) and biases (−3.3 to −10.5%) were not an improvement over just using the MTBS polygon (Table 1). This result was expected given the ecosystem is more suited to RdNBR.

Conclusions

To recap, the specific questions we sought to address for the MTBS area burned product were:

(1) What is the areal accuracy of the burned area MTBS polygons?
(2) Can the accuracy be improved by applying a simple threshold to spectral indices within the polygons?

In terms of (1), validation over four large fire events in a shrub–steppe environment showed that despite having high classification accuracies, the MTBS perimeters systematically overestimated the area burned, between 4 and 16.8% in the four validation sites. These findings suggest that caution is needed when area estimates derived from the MTBS burned area perimeters are used directly for scientific investigations (e.g. to evaluate burned area trends within temporal series). In terms of (2), this study shows that for shrub–steppe environments the area burned estimates can be significantly improved if a simple threshold on spectral index values is used within the MTBS perimeters. The CSI, RdNBR and MIRBI indices provide high accuracies (>90%), but require the estimation of a different optimal threshold for each fire and thus are not ideal within an automated system. The use of the dNBR unburned-to-low threshold provided by the MTBS metadata produced results that, albeit variable and not an improvement in accuracy across the four cases, are very close to the results obtained with the spectral indices.

A simple but effective route to improve the MTBS burned area perimeter product would be to apply a spectral index optimised to discriminate burned and unburned surfaces to the pixels within the MTBS burned area polygon. The steps to achieve this could include:

(1) Subset the original Landsat imagery by the MTBS burned area perimeter product but ensure that a similar quantity of unburned and burned pixels are present (i.e. equal class sizes).
(2) The spectral indices should then be selected on a fire regime-specific basis from the available burned area mapping literature. These should not be severity indices, as these require classes to exhibit large variances, whereas burned area mapping classes should exhibit well-separated means with small variances (Lentile *et al.* 2009).
(3) If automation is desired, these indices should not require determination of case-specific optimal thresholds.
(4) If burned–unburned thresholds are not readily available for these different fire regimes, research will be needed to evaluate the most appropriate spectral indices and their optimal thresholds.
(5) If comprehensive reference imagery is not available, statistical sampling methods should be used (Olofsson *et al.* 2013, 2014).

In summary, this case study clearly demonstrates the need to extend MTBS validation assessments to other fire regimes and

to evaluate the potential of other burned area mapping spectral indices to improve the MTBS polygon estimates.

Acknowledgements

This work was partially funded by the National Aeronautics and Space Administration (NASA) under awards NNX11AO24G and NNX11AF19G. We especially thank Jay Miller, Stephen Howard and Joshua Picotte, who provided clarification on the use of RdNBR and the MTBS products.

References

Abatzoglou JT, Kolden CA (2011) Climate change in western US deserts: potential for increased wildfire and invasive annual grasses. *Rangeland Ecology and Management* **64**(5), 471–478. doi:10.2111/REM-D-09-00151.1

Abatzoglou JT, Kolden CA (2013) Relationships between climate and macroscale area burned in the western United States. *International Journal of Wildland Fire* **22**(7), 1003–1020. doi:10.1071/WF13019

Baker WL (2006) Fire and restoration of sagebrush ecosystems. *Wildlife Society Bulletin* **34**(1), 177–185. doi:10.2193/0091-7648(2006)34[177:FAROSE]2.0.CO;2

Boschetti L, Brivio PA, Eva HD, Gallego J, Baraldi A, Gregiore J-M (2006) A sampling method for the retrospective validation of global burned area products. *IEEE Transactions on Geoscience and Remote Sensing* **44**(7), 1765–1773. doi:10.1109/TGRS.2006.874039

Boschetti L, Roy DP, Justice CO (2009) International Global Burned Area Satellite Product Validation Protocol Part I – production and standardization of validation reference data (to be followed by part II – accuracy reporting). Available at http://lpvs.gsfc.nasa.gov/PDF/BurnedAreaValidationProtocol.pdf [Verified 8 October 2014]

Brewer CK, Winne JC, Redmond RL, Opitz DW, Mangrich MV (2005) Classifying and mapping wildfire severity: a comparison of methods. *Photogrammetric Engineering and Remote Sensing* **71**(11), 1311–1320. doi:10.14358/PERS.71.11.1311

Chambers JC, Roundy BA, Blank RR, Meyer SE, Whittaker A (2007) What makes Great Basin sagebrush ecosystems invasible by *Bromus tectorum*? *Ecological Monographs* **77**(1), 117–145. doi:10.1890/05-1991

Crawford JA, Olson RA, West NE, Mosley JC, Schroeder MA, Whitson TD, Miller RF, Gregg MA, Boyd CS (2004) Synthesis paper: ecology and management of sage-grouse and sage-grouse habitat. *Journal of Range Management* **57**(1), 2–19. doi:10.2307/4003949

Dillon GK, Holden ZA, Morgan P, Crimmins MA, Heyerdahl EK, Luce CH (2011) Both topography and climate affected forest and woodland burn severity in two regions of the western US, 1984 to 2006. *Ecosphere* **2**, 12, Article 130. doi:10.1890/ES11-00271.1

Eidenshink J, Schwind B, Brewer K, Zhu Z, Quayle B, Howard S (2007) A project for monitoring trends in burn severity. *Fire Ecology* **3**, 3–21. doi:10.4996/FIREECOLOGY.0301003

Heward H, Smith AMS, Roy DP, Tinkham WT, Hoffman CM, Morgan P, Lannom KO (2013) Is burn severity related to fire intensity? Observations from landscape scale remote sensing. *International Journal of Wildland Fire* **22**, 910–918. doi:10.1071/WF12087

Holden ZA, Smith AMS, Morgan P, Rollins MG, Gessler PE (2005) Evaluation of novel thermally enhanced spectral indices for mapping fire perimeters and comparison with fire atlas data. *International Journal of Remote Sensing* **26**(21), 4801–4808. doi:10.1080/01431160500239008

Kolden CA, Lutz JA, Key CH, Kane JT, van Wagtendonk JW (2012) Mapped versus actual burned area within wildfire perimeters: characterizing the unburned. *Forest Ecology and Management* **286**, 38–47. doi:10.1016/J.FORECO.2012.08.020

Lannom KO, Tinkham WT, Smith AMS, Abatzoglou J, Newingham BA, Hall T, Morgan P, Strand EK, Paveglio Y, Anderson JW, Sparks AM (2014) Defining extreme wildland fires using geospatial and ancillary metrics. *International Journal of Wildland Fire* **23**, 322–337. doi:10.1071/WF13065

Lentile LB, Holden ZA, Smith AMS, Falkowski MJ, Hudak AT, Morgan P, Lewis SA, Gessler PE, Benson NC (2006) Remote sensing techniques to assess active fire characteristics and post-fire effects. *International Journal of Wildland Fire* **15**(3), 319–345. doi:10.1071/WF05097

Lentile LB, Smith AMS, Hudak AT, Morgan P, Bobbitt M, Lewis SA, Robichaud P (2009) Remote sensing for prediction of 1-year post-fire ecosystem condition. *International Journal of Wildland Fire* **18**, 594–608. doi:10.1071/WF07091

Lund GH (2007) Accounting for the world's rangelands. *Rangelands* **29**(1), 3–10. doi:10.2111/1551-501X(2007)29[3:AFTWR]2.0.CO;2

Masek JG, Vermote EF, Saleous NE, Wolfe R, Hall FG, Huemmrich KF, Gao F, Kutler J, Lim TK (2006) A Landsat surface reflectance dataset for North America, 1990–2000. *IEEE Geoscience and Remote Sensing Letters* **3**(1), 68–72. doi:10.1109/LGRS.2005.857030

Masek JG, Huang CQ, Wolfe R, Cohen W, Hall F, Kutler J, Nelson P (2008) North American forest disturbance mapped from a decadal Landsat record. *Remote Sensing of Environment* **112**(6), 2914–2926. doi:10.1016/J.RSE.2008.02.010

Miller JD, Thode AE (2007) Quantifying burn severity in a heterogeneous landscape with a relative version of the delta Normalized Burn Ratio (dNBR). *Remote Sensing of Environment* **109**, 66–80. doi:10.1016/J.RSE.2006.12.006

Morton DC, Collatz GJ, Wang D, Randerson JT, Giglio L, Chen Y (2012) Satellite-based assessment of climate controls on US burned area. *Biogeosciences* **9**, 7853–7892. doi:10.5194/BGD-9-7853-2012

Oliveira SLJ, Periera JMC, Carrieras JMB (2012) Fire frequency analysis in Portugal (1975–2005), using Landsat-based burnt area maps. *International Journal of Wildland Fire* **21**, 48–60. doi:10.1071/WF10131

Olofsson P, Foody GM, Stehman SV, Woosdock CE (2013) Making better use of accuracy data in land change studies: estimating accuracy and area and quantifying uncertainty using stratified estimation. *Remote Sensing of Environment* **129**, 122–131. doi:10.1016/J.RSE.2012.10.031

Olofsson P, Foody GM, Herold M, Stehman SV, Woodcock CE, Wulder MA (2014) Good practices for estimating area and assessing accuracy of land change. *Remote Sensing of Environment* **148**, 42–57. doi:10.1016/J.RSE.2014.02.015

Pereira JMC, Sá ACL, Sousa AMO, Silva JMN, Santos TN, Carreiras JMB (1999) Spectral characterisation and discrimination of burnt areas. In 'Remote Sensing of Large Wildfires in the European Mediterranean Basin', (Ed E Chuvieco) pp. 123–138 (Springer-Verlag: Berlin).

Petropoulos GP, Vadrevu KP, Xanthopoulos G, Karantounias G, Scholza M (2010) A comparison of spectral angle mapper and artificial neural network classifiers combined with Landsat TM imagery analysis for obtaining burnt area mapping. *Sensors* **10**, 1967–1985. doi:10.3390/S100301967

Picotte JJ, Robertson K (2011) Timing constraints on remote sensing of wildland fire burned area in the southeastern US. *Remote Sensing* **3**, 1680–1690. doi:10.3390/RS3081680

Randerson J. T., Chen Y., Werf G. R., Rogers B. M., Morton D. C. (2012) Global burned area and biomass burning emissions from small fires. *Journal of Geophysical Research: Biogeosciences* **117**(G4). doi:10.1029/2012JG002128

Riley KL, Abatzoglou JT, Greenfell IC, Klene AE, Heinsch FA (2013) The relationship of large fire occurrence with drought and fire danger indices in the western USA, 1984–2008: the role of temporal scale. *International Journal of Wildland Fire* **22**, 894–909. doi:10.1071/WF12149

Roy DP, Boschetti L, Justice CO, Ju J (2008) The collection 5 MODIS burned area product – global evaluation by comparison with the MODIS active fire product. *Remote Sensing of Environment* **112**, 3690–3707. doi:10.1016/J.RSE.2008.05.013

Smith AMS, Wooster MJ, Powell AK, Usher D (2002) Texture based feature extraction: application to burn scar detection in Earth Observation Imagery. *International Journal of Remote Sensing* **23**, 1733–1739. doi:10.1080/01431160110106104

Smith AMS, Wooster MJ, Drake NA, Dipotso FM, Perry GLW (2005) Fire in Africa savanna: testing the impact of incomplete combustion on pyrogenic emission estimates. *Ecological Applications* **15**(3), 1074–1082. doi:10.1890/03-5256

Smith AMS, Lentile LB, Hudak AT, Morgan P (2007*a*) Evaluation of linear spectral unmixing and dNBR for predicting post-fire recovery in a N. American ponderosa pine forest. *International Journal of Remote Sensing* **28**(22), 5159–5166. doi:10.1080/01431160701395161

Smith AMS, Drake NA, Wooster MJ, Hudak AT, Holden ZA, Gibbons CJ (2007*b*) production of Landsat ETM+ Reference imagery of burned areas within southern African savannahs: comparison of methods and application to MODIS. *International Journal of Remote Sensing* **28**(12), 2753–2775. doi:10.1080/01431160600954704

Stringham TK, Kruger WC, Shaver PL (2003) State and transition modeling: an ecological process approach. *Journal of Range Management* **56**(2), 106–113. doi:10.2307/4003893

Stroppiana D, Bordogna G, Carrara P, Boschetti M, Boschetti M, Brivio PA (2012) A method for extracting burned areas from Landsat TM/ETM plus images by soft aggregation of multiple Spectral Indices and a region growing algorithm. *ISPRS Journal of Photogrammetry and Remote Sensing* **69**, 88–102. doi:10.1016/J.ISPRSJPRS.2012.03.001

Sunderman SO, Weisberg PJ (2011) Remote sensing approaches for reconstructing fire perimeters and burn severity mosaics in desert spring ecosystems. *Remote Sensing of Environment* **115**, 2384–2389. doi:10.1016/J.RSE.2011.05.001

Trigg S, Flasse S (2001) An evaluation of different bi-spectral space for discriminating burned shrub-savannah. *International Journal of Remote Sensing* **22**(13), 2641–2647. doi:10.1080/01431160110053185

Verstraete MM, Pinty BP (1996) Designing optimal spectral indexes for remote sensing applications. *IEEE Transactions on Geoscience and Remote Sensing* **34**(5), 1254–1265. doi:10.1109/36.536541

West NE, Young JA (2000) Intermountain valleys and lower mountain slopes. In 'North American Terrestrial Vegetation', 2nd ed. (Eds MG Barbour, WD Billings) pp. 255–284. (Cambridge University Press: Cambridge, UK)

Zheng D, Heath LS, Ducey MJ, Smith JE (2011) Carbon changes in conterminous US forests associated with growth and major disturbances: 1992–2001. *Environmental Research Letters* **6**(1), 014012. doi:10.1088/1748-9326/6/1/014012